

# POWER-COMPENSATED SINGLE-CRYSTAL SILICON THERMOPILES FOR DIFFERENTIAL SCANNING CALORIMETRY (DSC)

Hao Jia<sup>1,2\*</sup>, Zhi Cao<sup>1,3</sup>, Zechun Li<sup>1,2</sup>, Haozhi Zhang<sup>1,2</sup>, Pengcheng Xu<sup>1,2</sup>, and Xinxin Li<sup>1,2\*</sup>

<sup>1</sup>State Key Lab of Transducer Technology, Shanghai Institute of Microsystem and Information Technology, Chinese Academy of Sciences, Shanghai 200050, CHINA

<sup>2</sup>University of Chinese Academy of Sciences, Beijing 100049, CHINA

<sup>3</sup>School of Chemical and Environmental Engineering, Shanghai Institute of Technology, Shanghai 201418, CHINA

## ABSTRACT

We demonstrate power-compensated MEMS thermopiles for chip-based differential scanning calorimetry (DSC). Different from the conventional DSC apparatus (using a pair of crucibles and macroscopic thermocouples) that suffers from low responsivity (~1-10 mV/W) and slow heating rates (~1-5°C/s), our MEMS differential thermopiles, integrated with 54 pairs of P-type/N-type single-crystal silicon thermocouples, offer outstanding power responsivity (~100V/W) and intrinsic heating rate of >10<sup>5</sup> °C/s. The temperature responsivity (28mV/°C) is also ~7 times higher than the commercialized devices (~4mV/°C). We then demonstrate rapid DSC measurement on indium melting. Proportional-integral-derivative (PID) control circuitry and algorithm are implemented for programmed heating rates up to 100°C/s. Simultaneously, another PID control scheme is employed for power compensation. We measure the latent heat of fusion for indium to be ~27.5J/g at 2 and 10°C/s, which agrees with the nominal value (28.53 J/g). Our MEMS thermopiles hold promise for quantitative analysis of endothermic /exothermic processes in various fields.

## KEYWORDS

MEMS thermopiles, differential scanning calorimetry (DSC), power compensation, indium melting

## INTRODUCTION

Differential scanning calorimetry (DSC) is an analytical technique for rapidly characterizing physical transformation, chemical reaction kinetics, etc. Conventionally, when the analyte is subjected to programmed heating (or cooling) in one crucible, and another crucible is left empty, the heat absorption (or release) could happen at a specific temperature (*i.e.*, characteristic temperature,  $T_c$ ), causing a differential output of a pair of thermocouples underneath the two crucibles. Different from the differential thermal analysis (DTA) which only measures  $T_c$ , DSC requires a power compensation circuit and algorithm to quantify the amount of heat absorption (or release) in units of J/g or W/g [1]. Due to the crucibles (sensing and reference) and macroscopic thermocouples, conventional DSC instruments suffer from low responsivity of ~1-10 mV/W and compromised heating rates of ~1-5°C/s, considering uniform sample heating [2]. Thanks to microfabrication technology, the heating and temperature sensing elements can be miniaturized onto a single device, leading to MEMS differential thermopile sensors. These devices offer better temperature and power sensitivity (*e.g.*, ~4mV/°C,

~24V/W) and a high heating rate (1°C/s~1000°C/s) [3-5].

To continuously push for high-performance DSC applications, the temperature responsivity of MEMS thermopiles needs to be further improved. Therefore, we have developed single-crystal silicon MEMS thermopile sensors with even higher temperature responsivity (28mV/°C) (7-fold improvement) [6-7] and DTA experiments have been conducted [8-9]. Nevertheless, it is highly demanded to realize a rapid and quantitative DSC technique by engineering power-compensated single-crystal silicon thermopiles.

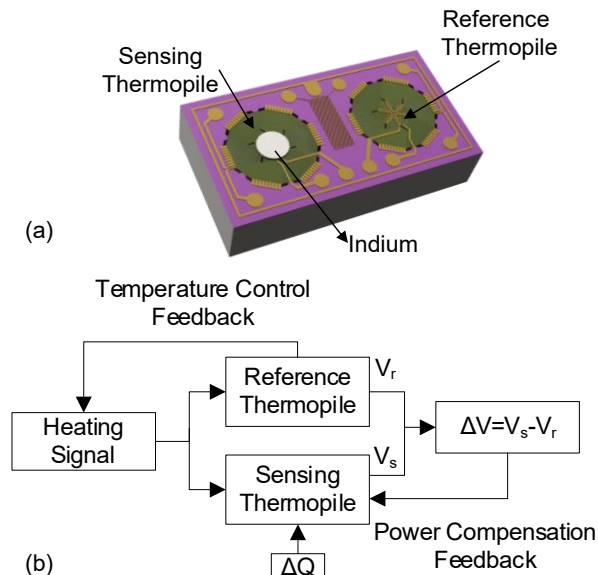


Figure 1: MEMS differential thermopiles for DSC characterization. (a) Schematic illustration of the single-crystal silicon differential thermopiles. The MEMS device consists of a sensing thermopile loaded with a sample (*e.g.*, indium in this work) and a reference thermopile. (b) Diagram of the power-compensated DSC system. The endothermic process of indium melting is quantified by combining temperature control and power compensation feedback circuits.

## SENSOR DESIGN

The DSC sensor consists of two identical thermopiles, as shown in Fig. 1a. Each thermopile is integrated with 54 pairs of single-crystal silicon thermocouples suspended over a ~640μm-diameter SiN<sub>x</sub> membrane. It is well known that the Seebeck coefficient of single-crystal silicon can be much higher than that of polysilicon [10]. On the other hand, increasing the number of thermocouples will lead to more accumulated thermoelectric voltages when arranged in series. A 240μm-diameter area in the thermopile center

is designed for sample loading. The hot junctions of the thermocouples are surrounded by the heating resistor in the sample loading region and the cold junctions are connected in parallel to the silicon frames, which share the same ambient temperature.

As shown in Fig. 1b, given metal (indium, In) melting as an example, the programmed heating is controlled by a temperature control feedback circuit, and when melting-induced heat absorption ( $\Delta Q$ ) happens at  $T_c=156.6^\circ\text{C}$ , the differential output ( $\Delta V=V_s-V_r$ ) will not be 0, and power-compensation via feedback circuit will add more heating power to the sensing thermopile, to balance  $V_s$  and  $V_r$  to maintain  $\Delta V=0$ .

## EXPERIMENTAL SYSTEM

Figure 2 shows the experimental system for DSC measurements. The MEMS thermopile device is wire-bonded to the PCB board. Thanks to the miniature size, the chip could be readily placed under an optical microscope, such that the morphology change of the analyte is recorded during DSC characterization. We develop PID control circuitry and algorithm and optimize it for programmed heating rates up to  $100^\circ\text{C}/\text{s}$ . The power compensation is implemented by another high-speed PID. Take indium melting as an example, the heat absorption and power compensation happen on the order of  $\sim 100\text{ms}$  at heating rates  $1\text{-}10^\circ\text{C}/\text{s}$ . Therefore, our high-speed PID modules can dynamically compensate the power applied to the sensing thermopile, to maintain  $\Delta V=0$ .

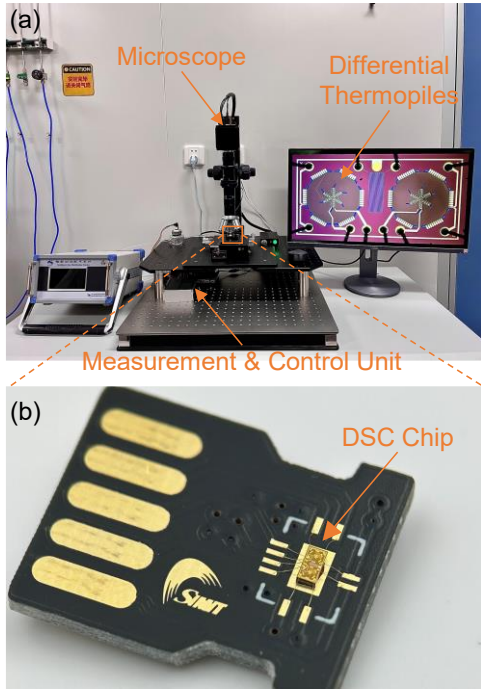


Figure 2: Experimental system. (a) Optical image of the system combining a DSC measurement & control unit and an optical microscope to monitor the morphology change of the sample. (b) Zoom-in view of a typical wire-bonded DSC chip under the microscope.

## DEVICE CHARACTERIZATION

We first characterize the temperature sensitivity of the MEMS thermopiles before DSC measurements. As shown

in Fig. 3a, when we apply a heating voltage ( $V_h$ ) to the heating resistor, the center of a single thermopile is uniformly heated. Thus, we can measure the temperature values ( $T$ ) at different heating voltages to calibrate the  $T$  vs.  $V_h$  curve, as shown in Fig. 3b. The measured curve also shows good agreement with the finite element modeling result, confirming the design of the MEMS thermopile devices. We then calibrate the output voltages of a single thermopile at different heating temperature values ( $V_{out}$  vs.  $T$ ). Hence, the temperature sensitivity is measured to be  $\alpha \sim 28\text{mV}/^\circ\text{C}$ , as shown in Fig. 3c, which is  $\sim 7$  times better than the current differential MEMS thermopiles [4].

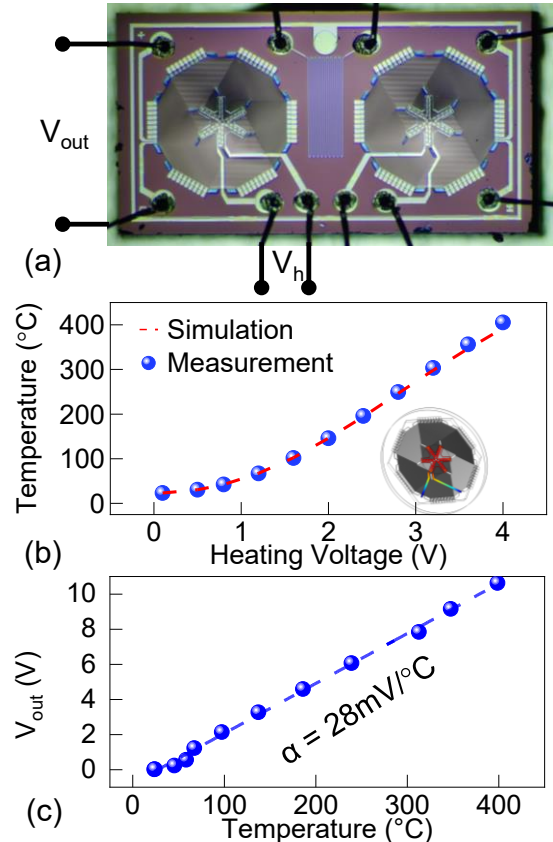


Figure 3: Temperature sensitivity of the MEMS thermopiles. (a) Single thermopile (e.g., sensing thermopile) is heated by  $V_h$  and the temperature ( $T$ ) and output voltage ( $V_{out}$ ) are measured. (b) Simulated and measured temperature values at different heating voltages ( $T$  vs.  $V_h$ ). (c) Output voltages at different heating temperature values ( $V_{out}$  vs.  $T$ ). The temperature sensitivity is measured to be  $\alpha \sim 28\text{mV}/^\circ\text{C}$ .

We also measure the dynamic thermal response of the MEMS thermopiles when subjected to the step heating/cooling, which is critical for designing PID parameters. As shown in Fig. 4a-d, we set a heating step of  $400^\circ\text{C}$  for a single thermopile, and measure a response time of  $\tau_{90} = 7.2$  ms and a maximum heating rate up to  $1.2 \times 10^5\text{^\circ C/s}$ . Similarly, for step cooling, the thermopile exhibits a response time of  $\tau_{90} = 7.4$  ms and a maximum heating rate of up to  $1.2 \times 10^5\text{^\circ C/s}$ . Overall, our MEMS differential thermopiles can support high-speed temperature control and power compensation for DSC applications in the next section.

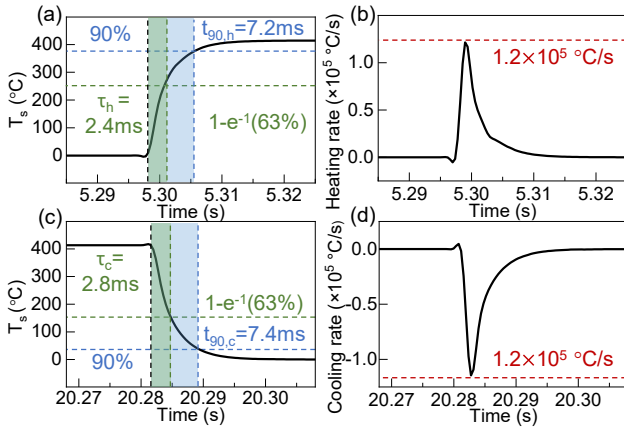


Figure 4: Temperature response of the MEMS thermopiles. (a-d) The measured temperature responses show a heating/cooling response time of <10ms and a maximum heating/cooling rate of  $>1 \times 10^5 \text{ }^\circ\text{C/s}$ .

## RESULTS AND DISCUSSION

Figure 5a shows the signal transduction of the DSC chip with temperature control PID and power compensation PID. Each PID contains 3 parameters (namely,  $K_p$ ,  $K_i$ , and  $K_d$ ).  $H(s)$  is the transfer function of a single thermopile under step heating, which is experimentally measured and fitted by MATLAB toolbox. As to temperature control PID, three parameters are optimized such that the heating signal applied to both thermopiles (blue solid lines) should exactly follow the set values (red dashed lines) at high rates. The results in Fig. 5b show that before optimization, the actual heating signal (at a heating rate of 100°C/s) cannot follow the set values. In contrast, after optimization, the actual heating signal (at a heating rate of 100°C/s) fully agrees with the set values.

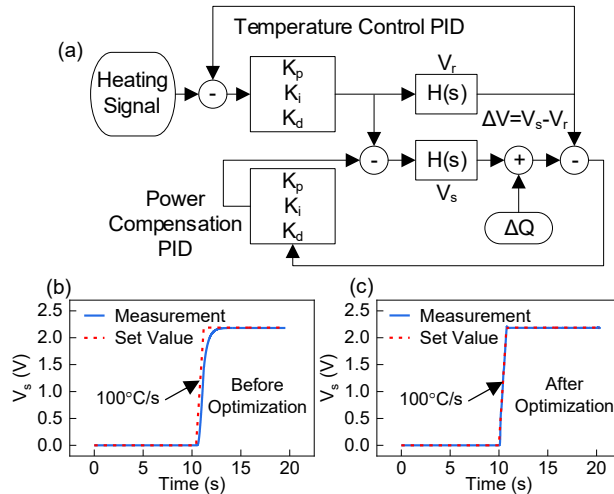


Figure 5: Temperature control and power compensation PIDs for DSC measurement. (a) Diagram of the temperature control PID and power compensation PID. (b-c) Optimization of temperature control PID at a heating rate of 100°C/s.

As to power compensation, the PID parameters are also optimized such that the differential voltage output remains 0. A piece of indium is cut by a razor blade and transferred to the center of the sensing thermopile by using

a micropipette. Using the microscope image, we estimate the area of the loaded sample to be  $\sim 0.018 \text{ mm}^2$  and an average thickness of  $\sim 150 \mu\text{m}$  (estimated mass  $\sim 20 \mu\text{g}$ ). Figure 6a shows the DTA curve for indium melting (without power compensation). At a heating rate of 10°C/s from room temperature to 200°C, we observe a sudden drop in the differential output signal ( $V_{\text{diff}} = V_s - V_r$ ), corresponding to the indium melting-induced heat absorption. After optimizing the power compensation PID,  $\Delta V$  remains almost 0, meaning that heat absorption is compensated by the PID. We still see a very small spike which corresponds to the most abrupt change in the DTA curve. The duration is only  $\sim 0.02\text{s}$ , almost the time taken by one cycle of the whole measurement and control circuit. This can be omitted compared with the time scale of the measured power compensation signal for indium melting ( $\sim 0.37\text{s}$  at 10°C/s,  $\sim 0.81\text{s}$  at 2°C/s) in Fig. 7.

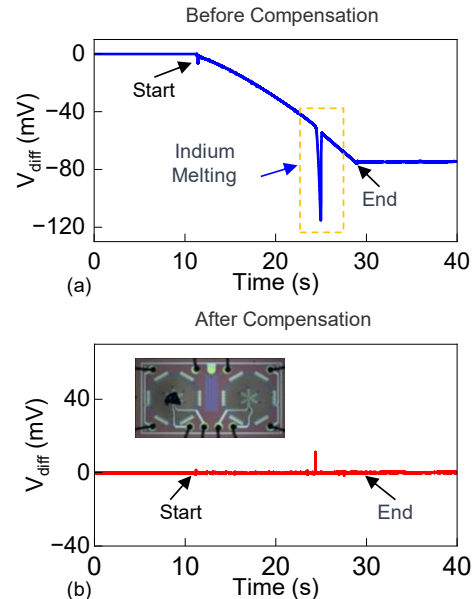
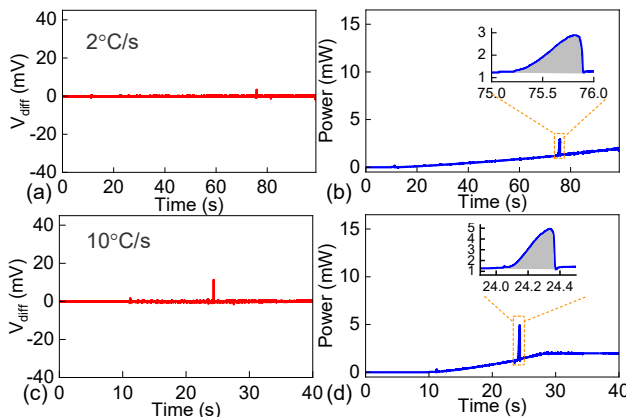


Figure 6: Power compensation of indium melting-induced heat absorption at a heating rate of 10°C/s. (a) Before power compensation,  $\Delta V$  shows the DTA curve of indium melting with a clear absorption peak. (b) After power compensation,  $\Delta V$  remains almost 0, meaning heat absorption is compensated by the PID.

With the optimized temperature control PID and power compensation PID, we then demonstrate the quantitative measurement of the latent heat of fusion for indium melting. We carry out the DSC measurement at 2 different heating rates of 2°C/s and 10°C/s. As shown in Fig. 7a and 7c, the differential output voltage remains almost 0, meaning that heat absorption is compensated by the PID. Figures 7b and 7d show the measured heating power of the sensing thermopile, and we can observe the compensated power on top of the background. The background is a baseline due to the mismatch between the sensing and reference thermopiles. The differential thermopiles cannot be identical due to the fabrication, on the other hand, the baseline can be subtracted by a measurement cycle before sample loading. When zooming into the compensated power signal (gray areas), we can obtain the compensated energy due to indium melting by an integral over the horizontal axis (time). Overall, we

estimate  $\sim 0.55\text{mJ}$  at both heating rates of  $2$  and  $10^\circ\text{C/s}$ . Given the estimated indium sample mass to be  $\sim 20\text{ng}$ , we can calculate the latent heat of fusion to be  $\sim 27.5\text{J/g}$ , which agrees with the nominal value of  $\sim 28.53\text{ J/g}$  [11].



*Figure 7: DSC measurement of indium melting. At heating rates of (a-b)  $2^\circ\text{C/s}$  and (c-d)  $10^\circ\text{C/s}$ , the differential output signals (red) remain almost 0 due to power compensation. The compensated energy (blue) is measured to be  $\sim 0.55\text{mJ}$  in both cases (gray areas show power integral over time).*

## CONCLUSION

In summary, we have demonstrated power-compensated MEMS thermopiles for high-performance differential scanning calorimetry (DSC). The MEMS thermopile sensors are integrated with 54 pairs of single crystal thermocouples, which exhibit a very-high temperature sensitivity of  $\sim 28\text{mV/}^\circ\text{C}$  and a heating/cooling rate of  $>10^\circ\text{C/s}$ . We then implement temperature control PID and power compensation PID for the MEMS differential thermopiles, allowing us to perform a high-speed temperature ramp of up to  $100^\circ\text{C/s}$ , and compelling power compensation up to  $10^\circ\text{C/s}$  for characterizing the metal melting process. Moreover, by using our DSC chip, we quantify the latent heat of fusion for indium to be  $\sim 27.5\text{J/g}$ , which agrees with the nominal value of  $\sim 28.53\text{ J/g}$ . Our high-sensitivity MEMS differential thermopiles hold promise for the quantitative characterization of physical and thermodynamic processes in different fields.

## ACKNOWLEDGEMENTS

The authors acknowledge financial support from the National Key R&D Program of China (2021YFB3200800), the National Natural Science Foundation of China (62227815, 61974155, 61831021, 62271473, 62104241, U21A20500), the Innovation Team and Talents Cultivation Program of the National Administration of Traditional Chinese Medicine (ZYYCXTD-D-202002, ZYYCXTD-D-202003).

## REFERENCES

- [1] P. J. Haines, M. Reading, and F. W. Wilburn, “Chapter 5 - Differential Thermal Analysis and Differential Scanning Calorimetry”, in *Handbook of Thermal Analysis and Calorimetry*, vol. 1, M. E. Brown, Ed. Elsevier Science B.V., 1998, pp. 279–361.
- [2] F. Schubert, M. Gollner, J. Kita, F. Linseis, and R. Moos, “First Steps to Develop a Sensor for a Tian-Calvet Calorimeter with Increased Sensitivity”, *J. Sens. Sens. Syst.*, vol. 5, no. 1, pp. 205–212, 2016.
- [3] A. W. van Herwaarden, “Overview of Calorimeter Chips for Various Applications”, *Thermochim. Acta.*, vol. 432, no. 2, pp. 192–201, 2005.
- [4] S. van Herwaarden, E. Iervolino, F. van Herwaarden, T. Wijffels, A. Leenaers, and V. Mathot, “Design, Performance and Analysis of Thermal Lag of the UFS1 Twin-Calorimeter Chip for Fast Scanning Calorimetry using the Mettler-Toledo Flash DSC 1”, *Thermochim. Acta.*, vol. 522, no. 1, pp. 46–52, 2011.
- [5] O. Nakabeppu, and K. Deno, “Nano-DTA and Nano-DSC with Cantilever-Type Calorimeter”, *Thermochim. Acta.*, vol. 637, pp. 1–10, Aug. 2016.
- [6] H. Zhang, H. Jia, Z. Ni, M. Li, Y. Chen, P. Xu, and X. Li, “1ppm-Detectable Hydrogen Gas Sensors by Using Highly Sensitive P+/N+ Single-Crystalline Silicon Thermopiles”, *Microsyst. Nanoeng.*, vol. 9, no. 1, art. no. 1, 2023.
- [7] H. Zhang, H. Jia, M. Li, P. Xu, and X. Li, “MEMS Differential Thermopiles for High-Sensitivity Hydrogen Gas Detection”, *2023 IEEE 36th International Conference on Micro Electro Mechanical Systems (MEMS)*, Munich, Germany, Jan. 2023, pp. 119–122.
- [8] H. Zhang, H. Jia, W. Feng, Z. Ni, P. Xu, and X. Li, “Ultra-Responsive MEMS Sensing Chip for Differential Thermal Analysis (DTA)”, *Sensors*, vol. 23, no. 3, art. no. 1362, 2023.
- [9] H. Zhang, H. Jia, W. Feng, P. Xu, and X. Li, “High-Responsivity Single-Crystal Silicon MEMS Thermopiles for Differential Thermal Analysis (DTA)”, *22nd International Conference on Solid-State Sensors, Actuators, and Microsystems (Transducers 2023)*, Kyoto, Japan, Jun. 2023.
- [10] J. Xie, C. Lee, M.-F. Wang, Y. Liu, and H. Feng, “Characterization of Heavily Doped Polysilicon Films for CMOS-MEMS Thermoelectric Power Generators”, *J. Micromech. Microeng.*, vol. 19, no. 12, art. no. 125029, 2009.
- [11] D. G. Archer, and S. Rudtsch, “Enthalpy of Fusion of Indium: A Certified Reference Material for Differential Scanning Calorimetry”, *J. Chem. Eng. Data*, vol. 48, no. 5, pp. 1157–1163, 2003.

## CONTACT

H. J. and Z. C. contributed equally to this work.  
\*H. Jia; hao.jia@mail.sim.ac.cn  
\*X. Li; xxli@mail.sim.ac.cn